Extensive dissolution of live pteropods in the Southern Ocean

N. Bednaršek[1,2,3], G. A. Tarling[1]*, D. C. E. Bakker[2], S. Fielding[1], E. M. Jones[4], H. J. Venables[1], P. Ward[1], A. Kuzirian[5], B. Lézé[2], R. A. Feely[6] and E. J. Murphy[1]

The carbonate chemistry of the surface ocean is rapidly changing with ocean acidification, a result of human activities[1]. In the upper layers of the Southern Ocean, aragonite—a metastable form of calcium carbonate with rapid dissolution kinetics—may become undersaturated by 2050 (ref. 2). Aragonite undersaturation is likely to affect aragonite-shelled organisms, which can dominate surface water communities in polar regions[3]. Here we present analyses of specimens of the pteropod *Limacina helicina antarctica* that were extracted live from the Southern Ocean early in 2008. We sampled from the top 200 m of the water column, where aragonite saturation levels were around 1, as upwelled deep water is mixed with surface water containing anthropogenic CO_2. Comparing the shell structure with samples from aragonite-supersaturated regions elsewhere under a scanning electron microscope, we found severe levels of shell dissolution in the undersaturated region alone. According to laboratory incubations of intact samples with a range of aragonite saturation levels, eight days of incubation in aragonite saturation levels of 0.94–1.12 produces equivalent levels of dissolution. As deep-water upwelling and CO_2 absorption by surface waters is likely to increase as a result of human activities[2,4], we conclude that upper ocean regions where aragonite-shelled organisms are affected by dissolution are likely to expand.

Aragonite skeletons and tests are important components of the oceanic carbon system because they contribute a significant fraction of the global flux of particulate calcium carbonate ($CaCO_3$) settling to the ocean floor[5]. They are especially important in the short-term buffering of the ocean absorption of anthropogenic CO_2 (refs 6,7). The surface ocean is generally saturated with respect to aragonite, that is, the aragonite saturation state (Ω_A) is greater than 1. However, the level of saturation decreases with depth. The point at which Ω_A falls below 1 is called the saturation horizon, and this generally occurs around 1,000 m but has shoaled by between 40 and 200 m as a direct consequence of the uptake of anthropogenic CO_2 (refs 2,8). Dissolution of shelled organisms mainly occurs when Ω falls below 1 but it has also been found in pteropods incubated in conditions where Ω_A was ≈ 1 (refs 9,10).

There are already reports of surface waters occasionally being undersaturated with respect to aragonite, including those of the Arctic Basin in 2008 after extensive melting of sea ice[11] and along the California continental shelf after seasonal upwelling of deep water[1]. South of the polar front in the Southern Ocean, winter cooling and strong persistent winds are
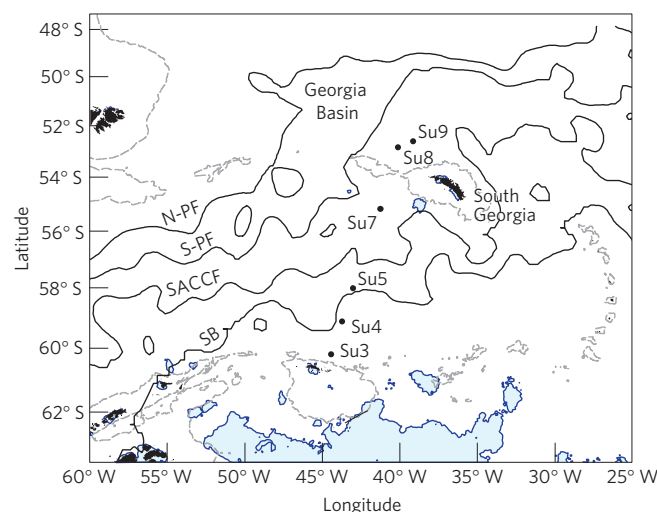

Figure 1 | Scotia Sea showing sampling station positions and frontal positions at time of sampling. Dynamic height contours were used to determine the location of the following fronts: SB, Southern Boundary; SACCF, Southern Antarctic Circumpolar Current Front; south and north edge of Polar Front (S-PF, N-PF). Fifteen per cent ice cover is represented by blue shading.

believed to be responsible for the ventilation of deeper waters to the surface, resulting in a natural decrease of carbonate ions of approximately 25% (35 µmol kg^{-1}) relative to summer[12]. When combined with increases in anthropogenic CO_2, ocean models predict that the Southern Ocean will begin to experience widespread aragonite undersaturation in surface waters after the year 2050 (refs 2,13).

Euthecosome pteropods are among a small number of taxa that make their shells principally from aragonite. The effects of Ω_A undersaturation on pteropods have mainly been investigated by laboratory incubations under enhanced partial pressures of CO_2 (pCO_2), simulating future atmospheric CO_2 scenarios. Pteropods have been found to exhibit shell malformations[14], lower rates of $CaCO_3$ precipitation[15] and dissolution of the shell exterior[2]. Effects have also been described on dead specimens collected in deep sediment traps[16], where shells exposed to aragonite undersaturation had an opaque and pitted appearance. It was demonstrated that sinking dead pteropods dissolved rapidly as they dropped below the

[1]British Antarctic Survey, Natural Environment Research Council, High Cross, Madingley Road, Cambridge, CB3 0ET, UK, [2]School of Environmental Sciences, University of East Anglia, Norwich Research Park, Norwich NR4 7TJ, UK, [3]University of Nova Gorica, Vipavska 13, 5000 Nova Gorica, Slovenia, [4]Royal Netherlands Institute for Sea Research, PO Box 59, 1790 AB Den Burg, Texel, The Netherlands, [5]Department of Geology and Geophysics, Woods Hole Oceanographic Institution, Woods Hole, Massachusetts 02543, USA, [6]NOAA, Pacific Marine Environmental Laboratory, Seattle, Washington 98115, USA. *e-mail: gant@bas.ac.uk.
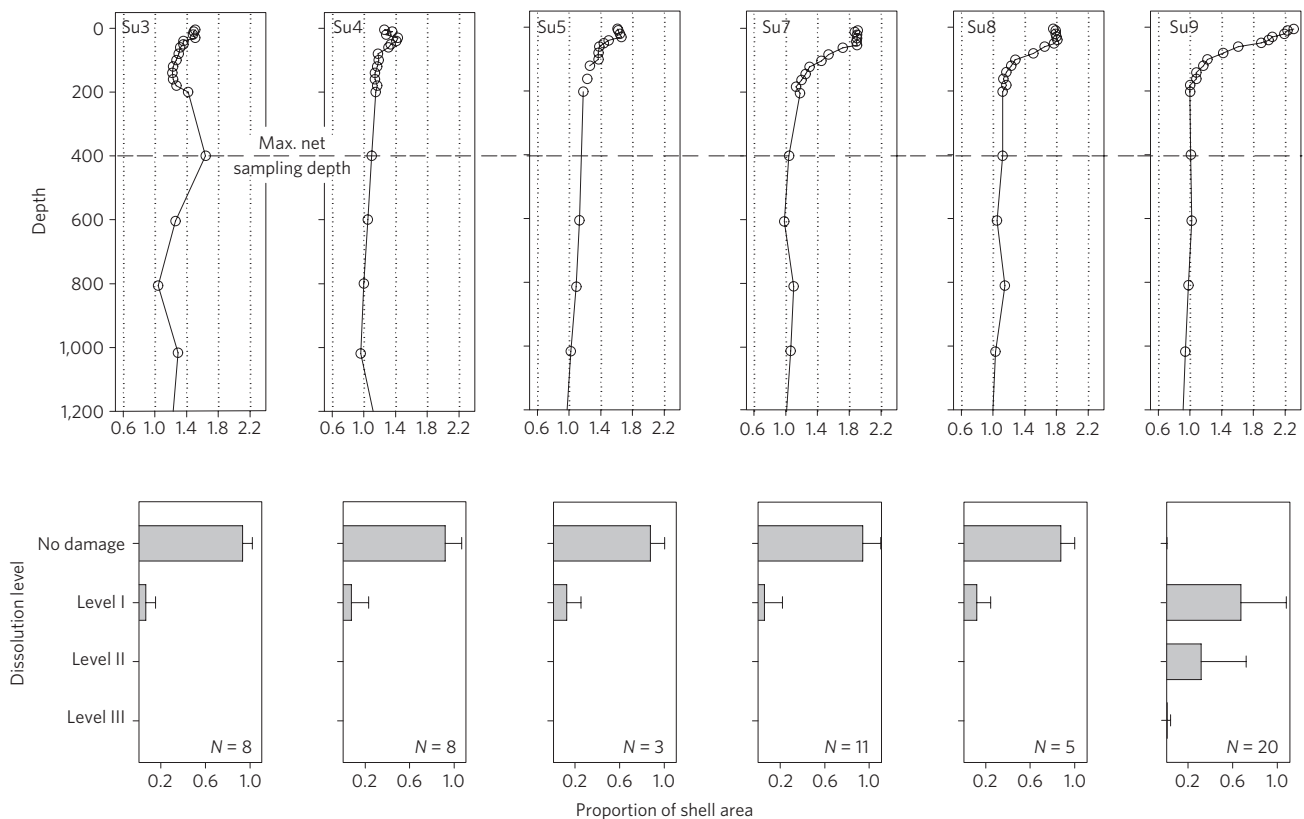
Figure 2 | Vertical profiles of Ω_A across the Scotia Sea (upper) and corresponding dissolution levels in live juvenile *L. helicina antarctica* (lower). *N* is the number of individuals analysed per station. The horizontal bars denote mean proportional shell area per dissolution level across all specimens; error bars represent 1 s.d. Level I dissolution was significantly higher in Su9 specimens compared with all other stations (Mann–Whitney rank sum test, $T = 778$, 20 and 35 df, $P < 0.001$). Su9 was also the only station in which level II and III dissolution was observed.
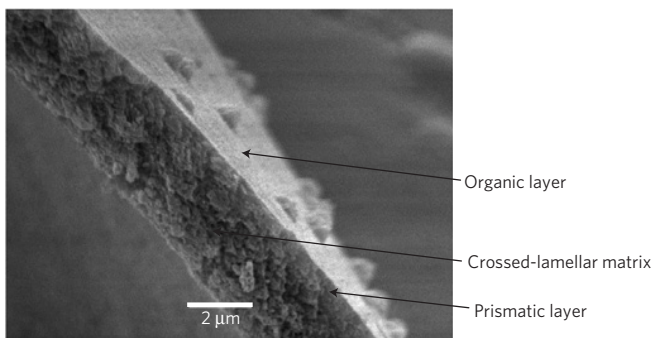

Figure 3 | SEM section of the shell of *L. helicina antarctica* showing the organic layer (periostracum), prismatic layer and crossed-lamellar matrix of aragonite crystals.

saturation horizon[9]. Furthermore, it was found that dissolution in dead specimens starts at Ω_A levels at or just below 1 across a range of North Pacific pteropod communities[10]. Until the present study, such effects have not been documented on live animals extracted directly from the natural environment.

Sampling was carried out in the Scotia Sea, located in the Atlantic Sector of the Southern Ocean, where the strong flow of the Antarctic Circumpolar Current is constricted in width. It is a physically dynamic region where deep-water upwelling occurs[17] and eddies from frontal regions are frequently encountered[18]. The interaction of strong Antarctic Circumpolar Current flows coupled with bottom topography leads to greater micronutrient availability and hence extensive phytoplankton blooms downstream of topographic features[19,20].

Live pteropods from this region were collected in January and February 2008 during cruise JR177 on RRS *James Clark Ross* as part of the British Antarctic Survey Discovery 2010 programme. Water sampling and depth-discrete net catches of mesozooplankton to 400 m were carried out along a south to north transect within the Scotia Sea (Fig. 1). The saturation horizon for aragonite was 1,000 m across most of the transect. However, at station Su9 (52.6° S, 39.1° W), there was a notable incursion of waters with low Ω_A values (minimum of 0.997) into layers above 400 m (Fig. 2).

L. helicina antarctica dominates mesozooplankton biomass in a number of Southern Ocean regions where it is the principle calcifying organism[21]. It is most commonly found above 400 m depth, particularly concentrating in the layers between 200 m and the surface[3]. It has a life cycle that can last upwards of 2 years, in which time it grows to 1 cm in shell diameter[21]. Analysis was carried out on both freshly caught material preserved directly on collection and on specimens that were incubated under manipulated CO_2 levels (375–750 ppm at 4 °C) to establish a response index. All freshly caught and incubated specimens were preserved in 70% ethanol. Subsequently, they were treated to dehydrate shell layers (Fig. 3) and to remove the periostracum (Fig. 4a,b) so that the state of the underlying shell matrix could be examined using scanning electron microscopy (SEM).

Different degrees of dissolution were identified in incubated shells of live pteropods (see Supplementary Information). We categorized them into three main levels according to the degree of encroachment on the upper prismatic layer and into the upper shell layer (Fig. 4). Specimens were scored blind and then correlated back to the experimental conditions. Incubations in which even only a slight degree of undersaturation was experienced for 8 d (Ω_A 0.94–1.12, pCO_2 of 675 μatm) were sufficient to cause substantial
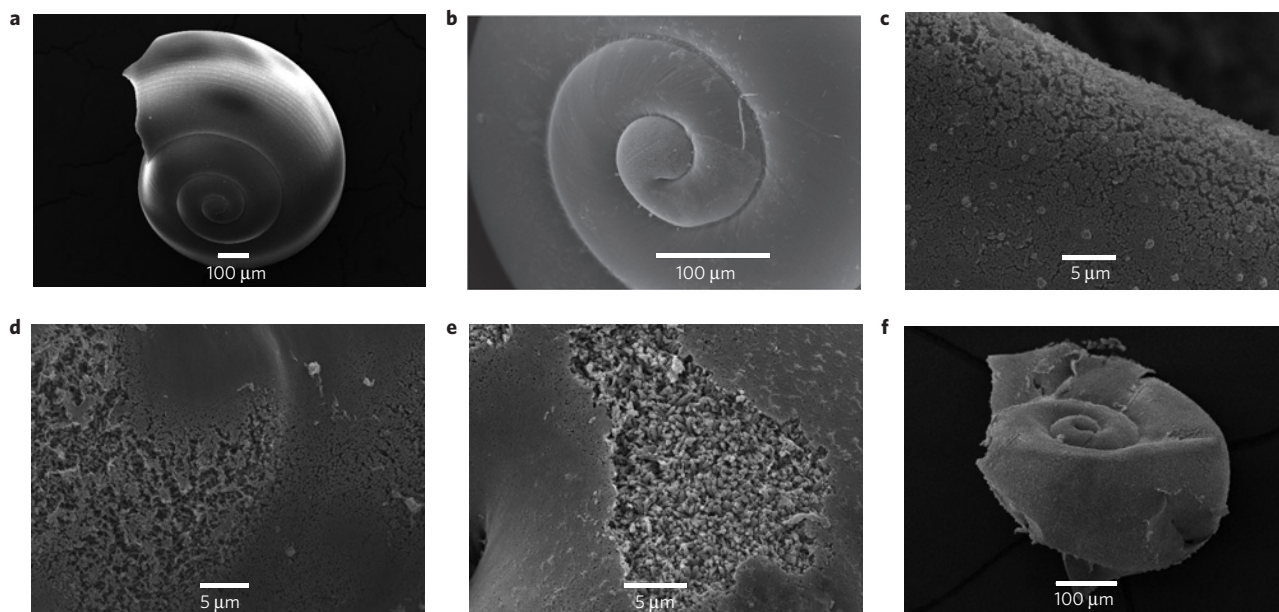
Figure 4 | SEM images of juvenile *L. helicina antarctica* (from which the periostracum has been removed) showing different levels of dissolution.
a,b, Intact animal without any indications of dissolution. **c**, Level I: the upper prismatic layer slightly dissolved. **d**, Level II: the prismatic layer partially or completely missing and the cross-lamellar matrix partially exposed with increasing porosity in the upper crystalline layer. **e,f**, Level III: the crossed-lamellar matrix showing signs of dissolution across large areas of the shell, and the shell becoming more fragile owing to fragmentation (high-resolution images are available in the Supplementary Information).

dissolution of the shell matrix relative to the supersaturated control (Ω_A 1.62–1.78, Fig. 5). We then examined freshly caught material, preserved directly on collection, for signs of such shell dissolution.

L. helicina antarctica juveniles were found at all sampling stations, with northern stations (<57° S) containing higher abundances (7.2×10^4–3.4×10^4 ind. m^{-2}) than those to the south (>57° S; 2.9×10^2–1.9×10^3 ind. m^{-2}). At station Su9, we found that *L. helicina antarctica* juvenile specimens contained all three levels of dissolution. Juveniles from other stations contained only small patches of the least severe level of dissolution (Figs 2 and 5), probably caused by Ω_A-undersaturated microenvironments close to the exterior surface resulting from the remineralization of organic matter[22].

Dissolution of live specimens from Su9 was apparent over the entirety of their shells as opposed to just the growing edge. This indicates first that the periostracum (the outer organic layer) provides little if any protection to the underlying shell matrix in juveniles. If it did so, then the growing edge, where the periostracum is thinnest, would have been more affected. Second, dissolution must have occurred recently; otherwise it would have been apparent also on the oldest, inner whorls and not only at the newly deposited growing parts of the shells. We conclude that the observed dissolution was principally a physico-chemical response to the carbonate chemistry conditions in a body of water inhabited for 4–14 d. The dissolution response is similar to other studies that incubated dead specimens at $\Omega_A \approx 1$ (refs 9,10), underlining the fact that live specimens have little to protect themselves from the effects of Ω_A undersaturation. Furthermore, in both live and dead specimens, it is apparent that dissolution can occur rapidly even when in just close proximity to the aragonite saturation horizon.

Regions of upwelling that bring the saturation horizon close to the surface are likely to be repeated through much of the Southern Ocean and are not a modern phenomenon[12]. These deep waters probably came into contact with the atmosphere around 1,000 years ago and so are unlikely to contain any anthropogenic CO_2. Mixing with surface waters will normally increase Ω_A to above saturation levels but increases in surface concentrations of CO_2 will reduce the effect of this dilution. At station Su9, an Ω_A of around 1 was observed up to a depth of about 200 m despite mixing with surface water. Calculations of the effect of anthropogenic carbon mixing down from surface waters (see Supplementary Information) showed a reduction of Ω_A values of approximately 0.1 relative to pre-industrial values. Station Su9 was a site of comparatively high phytoplankton biomass (60–90 mg C m^{-3}; ref. 20). However, dissolved inorganic carbon (DIC) levels below 100 m were similar to another site with similar water mass properties but low phytoplankton biomass[20], indicating that extensive remineralization had not taken place and the carbon export had not significantly lowered values of Ω_A. Therefore, the primary causes of low Ω_A values observed in this instance were mainly from the addition of anthropogenic CO_2 in surface waters mixing with upwelled deep water.

Climate models project a continued intensification in Southern Ocean winds throughout the twenty-first century if atmospheric CO_2 continues to increase[4]. In turn, this will increase wind-driven upwelling and potentially make instances of deep water, undersaturated in aragonite penetrating into the upper mixed layers more frequent. Simultaneously, rising atmospheric concentrations of anthropogenic CO_2 will continue to reduce aragonite saturation levels in surface waters, particularly in polar regions[12]. Conditions such as observed at station Su9 are therefore likely to become more common in the Southern Ocean, making shell dissolution an increasing threat to pteropod populations.

Pteropods do not necessarily die as a result of dissolution. Calcification of the inside of the shell probably continues and, to some degree, counteracts the dissolution of the exterior of the shell. Nevertheless, the observed rapidity of the dissolution response means that, in the present instance, there would have been net loss of shell overall, as reported in other experimental manipulations[15]. The main consequence of such loss of shell is an increased vulnerability to predation and infection, which will in turn impact other parts of the food web[15]. A drop in their population size will affect the ocean's carbonate cycle given the important role of pteropods in balancing oceanic alkalinity budgets[7]. Rates of vertical
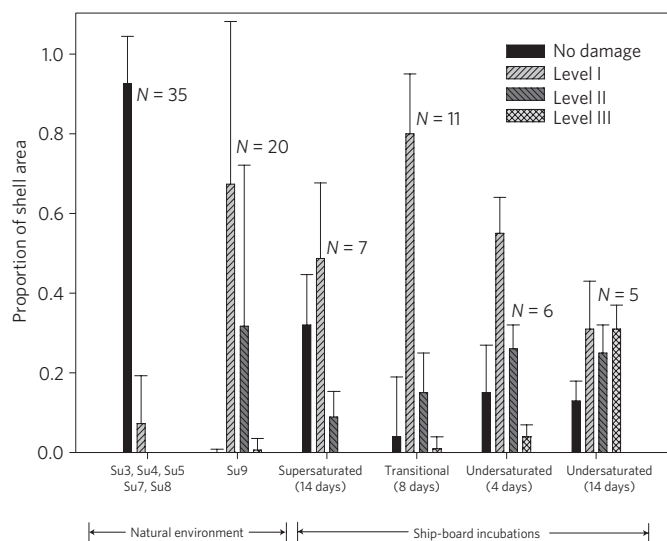
Figure 5 | Average (s.d.) proportion of different dissolution levels in live juvenile *L. helicina antarctica* from the natural environment and ship-board incubations. Supersaturated refers to $\Omega_A > 1.1$, transitional, 0.95-1.1 and undersaturated, 0.75-0.95. *N* refers to the numbers of specimens analysed. The vertical bars denote the mean proportional shell area per dissolution level; error bars represent 1 s.d. Incubation for 14 days in undersaturated conditions caused a significant increase in level III dissolution compared with all other groupings (Kruskal–Wallis one-way analysis of variance, $H = 51.7$, 4 df, $P < 0.001$). Extents of level II and III dissolution were statistically indistinguishable between Su9 and 8 day transitional incubations.

carbon flux will also decline, as the pteropod shells become less dense and less able to act as ballast for other particulate material[23].

This report documents a dissolution response of live juvenile pteropods within their natural environment as a result of exposure to waters where $\Omega_A \approx 1$. The data validate the prediction of a wide body of laboratory-based studies on the vulnerability of this important taxon to the acidification of polar oceans[2,14,24]. The shallow aragonite saturation horizon we observed was at least partially the result of oceanic absorption of anthropogenic CO_2 and demonstrates that the impact of ocean acidification is already occurring in oceanic populations, long before some projected dates of Ω_A undersaturation[12]. Regional declines of pteropod populations may occur sooner than projected at present as areas of Ω_A undersaturation in Southern Ocean surface waters become more widespread.

Methods

Field sampling. Samples were collected along a south to north transect within the Scotia Sea region of the Southern Ocean (60° S and 48° W–50° S 34° W, Fig. 1) in February 2008 on board the RRS *James Clark Ross*. Full-depth CTD (conductivity, temperature and depth) casts and plankton net samples were collected every 60 to 100 km along the transect. Water samples were collected every 50 m down to 200 m depth and then every 200 m down to 1,000 m depth during each CTD cast. Juvenile *L. helicina antarctica* were collected in the upper water column (0–400 m) with a vertically hauled motion compensated Bongo net (0.5m², 100 µm and 200 µm meshed nets). Captured specimens were either preserved immediately in 70% ethanol or used in incubation analyses.

Water analysis. Water samples were used for DIC and total alkalinity analysis following the Standard Operating Procedures for oceanic CO_2 measurements detailed in ref. 20. A VINDTA (Versatile Instrument for the Determination of Titration Alkalinity; Marianda) was used to measure DIC and total alkalinity, with a Certified Reference Material analysed in duplicate for DIC and total alkalinity at the beginning and end of each sample analysis day. The concentration of DIC was determined using the principles of coulometric analysis[25]. The accuracy of the DIC measurements was 2.4 µmol kg⁻¹ and the precision, 1.5 µmol kg⁻¹. Analysis for total alkalinity was carried out by potentiometric titration with hydrochloric acid to

the carbonic acid end point[26]. The accuracy and precision of total alkalinity values were 2.6 µmol kg⁻¹ and 1.0 µmol kg⁻¹, respectively.

DIC and total alkalinity, alongside temperature, salinity, pressure and macronutrient concentrations from all discrete samples, were used to calculate the remaining carbonate chemistry parameters including total pH (pH_T) and Ω aragonite (Ω_A). This was carried out using the CO_2 Sys programme[27] with thermodynamic dissociation constants for K_1 and K_2 from ref. 28 and the re-fit by ref. 29.

Pteropod analysis. Before further analysis, captured pteropod specimens were inspected to select only those that had not suffered mechanical damage during capture. Two sets of control samples were taken to consider capture and incubation effects—one immediately fixed post capture from an Ω_A supersaturated region (natural control), another after varying lengths of incubation in Ω_A supersaturated conditions ($\Omega = 1.7 \pm 0.08$; incubation control). There was no evidence of the more advanced stages of dissolution (levels II and III) in either the natural or incubation control samples. Level I dissolution covered just under 10% of the surface area in the natural control sample, and 56% of surface area in the incubation control, indicating an incubation effect. Accordingly, dissolution levels II and III were given most weight as indicators of dissolution when comparing incubated material with that taken directly from the natural environment.

Incubations were carried out in 0.22 GF/F filtered sea water to remove bacteria and held in 2 l blacked-out flasks through which was bubbled synthetic air containing one of four different CO_2 mixing ratios (xCO_2; BOC Special Products): 375, 500, 750 and 1,200 ppm (µmol mol⁻¹). Bubbling was stopped once water reached the correct CO_2 mixing ratio and around 50 individuals (principally juveniles) were introduced to the flask, which was subsequently sealed, with head space kept to a minimum. Incubations were run for between 4 and 14 d, with water samples taken at the start and end of each incubation to verify Ω_A state (as above). Accordingly, each flask was categorized into one of three Ω_A states: supersaturated (1.1–1.8), transitional (0.95-1.1) or under-saturated (0.75–0.95). All pteropods were preserved in 70% ethanol.

The preparation of preserved pteropod shells is described in detail in an accompanying publication[30]. Briefly, abiogenic crystal precipitates on the shell surface were removed with 6% hydrogen peroxide, followed by a dehydration method including the use of 2,2-dimethoxypropane and 1,1,1,3,3,3-hexamethyldisilazane. This procedure was finely tuned to remove the precipitates and dehydrate the specimens without damaging any shell layers. The overlying organic layer was then plasma-etched to expose the shell microstructure for SEM analysis, using a JEOL JSM 5900LV at an acceleration voltage of 15 kV and a working distance of about 10 mm. Fifteen to twenty SEM photographs were taken across the shell surface area of each specimen to determine the proportion of the shell surface covered by each level of dissolution. Each image was analysed using customized image-segmentation software (EDISON software) that estimated the extent of each dissolution level in each image. Images were combined to determine overall coverage for each specimen. A detailed description and user guidelines on the procedure are given at http://www.uea.ac.uk/~vtt07vju/segmentation/.

References

1. Feely, R. A., Sabine, C. L., Hernandez-Ayon, J. M., Ianson, D. & Hales, B. Evidence for upwelling of corrosive 'acidified' water onto the continental shelf. *Science* **320,** 1490–1492 (2008).
2. Orr, J. C. *et al.* Anthropogenic ocean acidification over the twenty-first century and its impact on calcifying organisms. *Nature* **437,** 681–686 (2005).
3. Hunt, B. P. V. *et al.* Pteropods in Southern Ocean ecosystems. *Prog. Oceanogr.* **78,** 193–221 (2008).
4. Le Quere, C. *et al.* Saturation of the Southern Ocean CO_2 sink due to recent climate change. *Science* **316,** 1735–1738 (2007).
5. Fabry, V. J. Shell growth rates of pteropod and heteropod molluscs and aragonite production in the open ocean: Implications for the marine carbonate system. *J. Mar. Res.* **48,** 209–222 (1990).
6. Broecker, W. S. & Takahashi, T. in *The Fate of Fossil Fuel CO_2 in the Oceans* (eds Andersen, N. R. & Malahoff, A.) 213–241 (1977).
7. Betzer, P. R. *et al.* The oceanic carbonate system—a reassessment of biogenic control. *Science* **226,** 1074–1077 (1984).
8. Feely, R. A. *et al.* Impact of anthropogenic CO_2 on the $CaCO_3$ system in the oceans. *Science* **305,** 362–366 (2004).
9. Byrne, R. H., Acker, J. G., Betzer, P. R., Feely, R. A. & Cates, M. H. Water column dissolution of aragonite in the Pacific Ocean. *Nature* **312,** 321–326 (1984).
10. Feely, R. A. *et al.* Winter-summer variations of calcite and aragonite saturation in the Northeast Pacific. *Mar. Chem.* **25,** 227–241 (1988).
11. Yamamoto-Kawai, M., McLaughlin, F. A., Carmack, E. C., Nishino, S. & Shimada, K. Aragonite undersaturation in the Arctic Ocean: Effects of ocean acidification and sea ice melt. *Science* **326,** 1098–1100 (2009).

12. McNeil, B. I. & Matear, R. J. Southern Ocean acidification: A tipping point at 450 ppm atmospheric CO_2. *Proc. Natl Acad. Sci. USA* **105,** 18860–18864 (2008).

13. Steinacher, M., Joos, F., Frolicher, T. L., Plattner, G. K. & Doney, S. C. Imminent ocean acidification in the Arctic projected with the NCAR global coupled carbon cycle-climate model. *Biogeosciences* **6,** 515–533 (2009).

14. Comeau, S., Jeffree, R., Teyssie, J. L. & Gattuso, J. P. Response of the Arctic pteropod *Limacina helicina* to projected future environmental conditions. *PLoS ONE* **5,** e11362 (2010).

15. Comeau, S., Gorsky, G., Alliouane, S. & Gattuso, J. P. Larvae of the pteropod *Cavolinia inflexa* exposed to aragonite undersaturation are viable but shell-less. *Mar. Biol.* **157,** 2341–2345 (2010).

16. Roberts, D. *et al.* Interannual pteropod variability in sediment traps deployed above and below the aragonite saturation horizon in the Sub-Antarctic Southern Ocean. *Polar Biol.* **34,** 1739–1750 (2011).

17. Heywood, K. J., Garabato, A. C. N. & Stevens, D. P. High mixing rates in the abyssal Southern Ocean. *Nature* **415,** 1011–1014 (2002).

18. Kahru, M., Mitchell, B. G., Gille, S. T., Hewes, C. D. & Holm-Hansen, O. Eddies enhance biological production in the Weddell-Scotia confluence of the Southern Ocean. *Geophys. Res. Lett.* **34,** L14603 (2007).

19. Park, J., Ohb, I-S., Kim, H-C. & Yoo, S. Variability of SeaWiFs chlorophyll-a in the southwest Atlantic sector of the Southern Ocean: Strong topographic effects and weak seasonality. *Deep-Sea Res Pt. I* **57,** 604–620 (2010).

20. Jones, E., Bakker, D., Venables, H. & Watson, A. Dynamic seasonal cycling of inorganic carbon downstream of South Georgia, Southern Ocean. *Deep-Sea Res. Pt. II* **59–60,** 25–35 (2012).

21. Bednarsek, N., Tarling, G., Fielding, S. & Bakker, D. Population dynamics and biogeochemical significance of *Limacina helicina antarctica* in the Scotia Sea (Southern Ocean). *Deep-Sea Res. Pt. II* **59–60,** 105–116 (2012).

22. Jansen, H., Zeebe, R.E. & Wolf-Gladrow, D.A. Modeling the dissolution of settling $CaCO_3$ in the ocean. *Glob. Biogeochem. Cycles* **16,** 1027 (2002).

23. Francois, R., Honjo, S., Krishfield, R. & Manganini, S. Factors controlling the flux of organic carbon to the bathypelagic zone of the ocean. *Glob. Biogeochem. Cycles* **16,** 1087 (2002).

24. Fabry, V. J., McClintock, J. B., Mathis, J. T. & Grebmeier, J. M. Ocean acidification at high latitudes: The bell weather. *Oceanography* **22,** 160–171 (2009).

25. Johnson, K. M., Sieburth, J. M., Williams, P. J. L. & Brandstrom, L. Coulometric total carbon dioxide analysis for marine studies—automation and calibration. *Mar. Chem.* **21,** 117–133 (1987).

26. Dickson, A. G. An exact definition of total alkalinity and a procedure for the estimation of alkalinity and total inorganic carbon from titration data. *Deep-Sea Res.* **28,** 609–623 (1981).

27. Lewis, E. & Wallace, D. W. R. *co2sys - Program Developed for CO_2 System Calculations* Report ORNL/CDIAC-105 (Carbon Dioxide Information and Analysis Centre, Oak Ridge Natl. Lab., US Dep. of Energy, 1998).

28. Mehrbach, C., Culberson, C. H., Hawley, J. E. & Pytkowicz, R. M. Measurement of the apparent dissociation constants of carbonic acid in seawater at atmospheric pressure. *Limnol. Oceanogr.* **18,** 897–907 (1973).

29. Dickson, A. G. & Millero, F. J. A comparison of the equilibrium constants for the dissociationof carbonic acid in seawater media. *Deep-Sea Res.* **34,** 1733–1743 (1987).

30. Bednarsek, N. *et al.* Description and quantification of pteropod shell dissolution: A sensitive bioindicator of ocean acidification. *Global Change Biol.* **18,** 2378–2388 (2012).

Author contributions

G.A.T. and D.C.E.B. conceived the project; N.B. carried out the fieldwork, with the assistance of G.A.T., S.F. and P.W.; E.M.J. and H.J.V. provided supporting environmental data; A.K. helped develop a method of shell preparation for SEM analysis; B.L. developed an image analysis method; G.A.T., N.B. and D.C.E.B. co-wrote the manuscript, with theoretical overviews provided by R.A.F. and all remaining authors commenting.

Additional information

Supplementary information is available in the online version of the paper. Reprints and permissions information is available online at www.nature.com/reprints. Correspondence and requests for materials should be addressed to G.A.T.

Competing financial interests

The authors declare no competing financial interests.